Euronoise 2018
Crete

Accuracy aspects for diffraction-based computation of scattering

U. Peter Svensson, Sara R. Martin, Jan Šlechta
Acoustics Research Centre, Department of Electronic Systems, Norwegian University of Science and Technology, Trondheim, Norway.

Jason E. Summers, Blake H. Teres, Charles F. Gaumond
ARiA, Washington DC, USA.

Summary
Edge-diffraction based modeling, in the form of the Edge Source Integral Equation (ESIE), [J. Acoust. Soc. Am. 133, pp. 3681-3691, 2013], has proven efficient and accurate for radiation problems such as modeling loudspeakers in convex-shaped rigid enclosures. Some singularity issues have been identified for certain source/receiver positions, and the problem as regards receiver positions can be avoided through a recently suggested hybrid technique [Proc. Meet. of Acoustics. 26, 015001, 2016]. The hybrid technique uses the edge-diffraction formulation to find the sound pressure at the surface of the scatterer, and employs the Kirchhoff-Helmholtz Integral Equation to propagate the surface sound pressure to external receiver points. For these techniques mentioned above, computed results are assumed to converge towards a correct result, and one usually has to use the finest mesh that is computable with the available resources. Such a single computation does, however, not directly indicate the accuracy of the result, but by employing computations for several mesh sizes, a Taylor expansion model of the computation error can offer the possibility for a Richardson extrapolation as a convergence acceleration technique. This technique is well-known for some computation techniques but possibly not so widely known. Here, this technique will be demonstrated for some particularly challenging cases of computing far-field backscattering at low frequencies from compact scatterers with the ESIE method, as well as some other challenging geometries. Pronounced cancellation effects between first- and higher-order diffraction components lead to very high accuracy requirements for the computations, and convergence acceleration turns out to be highly effective. [Portions of this material are based upon work supported by the Office of Naval Research under Contract No. N68335-17-C-0336; the Research Council of Norway, project no. 240278; and the ERCIM Alain Bensoussan Fellowship Programme].

PACS no. 43.20.Rz

1. Introduction

Scattering problems can be studied with a variety of techniques, including analytical solutions and numerical computation. The former exist only for a few canonical shapes, so numerical approaches typically must be used. These can be based on solving the wave equation, or using finite-element or finite-difference methods. For external scattering problems, such volume-element based methods might require large computational efforts due to the required domain discretization. A common alternative is the boundary element method (BEM), which is based on the Kirchhoff-Helmholtz integral equation (KHIE), which requires a discretization of the scattering body surface only. In this paper, an alternative approach is investigated: the decomposition of the scattered sound field into geometrical acoustics (GA) components and diffraction components of different orders. Such a decomposition can be made exact for a single infinite wedge by employing an exact diffraction expression. High-frequency asymptotic solutions such as the GTD or UTD are also commonly used, both for a single wedge, and for polyhedral bodies. Here, the edge source integral equation (ESIE) will be used for the modeling of higher-order diffraction. This model does not have the asymptotic limitations that GTD and UTD have, but it is also not clear how the solution relates to the true solution of the wave equation. The ESIE has been shown to give remarkably accurate results for the scattering from convex shaped bodies

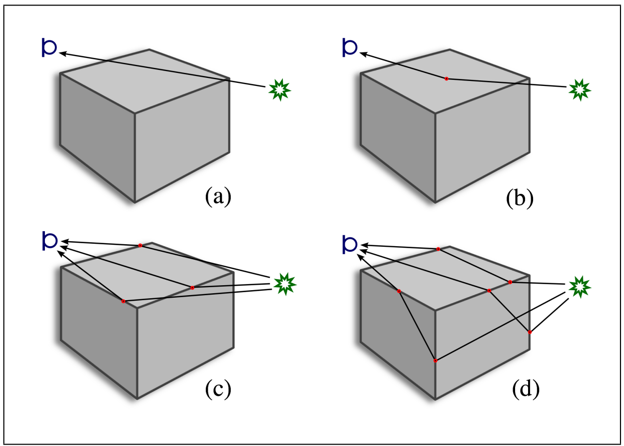

Figure 1. Illustration of the decomposition of the sound field into components: (a) Direct sound, (b) Specular reflection, (c) First-order diffraction, (d) Second-order diffraction

with rigid surfaces (the Neumann boundary condition). In this paper, the special case of back-scattering for low wavenumbers will be explored further since it is a numerically very challenging use for diffraction-based approaches.

2. Methods

2.1. Theory

The diffraction based approach decomposes the sound pressure at a receiver, p_{total}, as

$$p_{\text{total}} = p_{\text{GA}} + p_{\text{1. order diffraction}} + p_{\text{HOD}} \quad (1)$$

where p_{GA} represents the geometrical acoustics solution, that is, the direct sound + the specular reflection, and HOD stands for higher-order diffraction. It should be noted that the two GA components are both subject to visibility tests, which implies that a receiver behind a scattering object would have $p_{\text{GA}} = 0$. The diffraction terms of various orders are, as a consequence, also subject to visibility tests, so that the total sound field, p_{total}, is continuous everywhere. In Eq. (1), the grouping into first-order diffraction, and the accumulation of second-and-higher order diffraction, respectively, is a property of the ESIE. See Fig. 1 for an illustration of some of these terms.

2.2. Numerical implementation

The three terms in Eq. (1) are computed with different approaches. The GA components are available explicitly, with the direct sound on the form

$$p_{\text{direct}} = \frac{\mathrm{e}^{-\mathrm{j}kr}}{r} V_{\text{S,R}} \quad (2)$$

where k is the wavenumber, r is the distance from source to receiver, and $V_{\text{S,R}}$ is a visibility factor, being 1 if the line from S to R is unobstructed, 0 if the line obstructed, and 0.5 if the line is exactly hitting one edge. It could be pointed out that the expression in Eq. (2) is not exactly a sound pressure but rather a transfer function from a monopole source signal to the sound pressure at the receiver. The first-order diffraction is computed via numerical integration of integrals on the form given in [1]. Such an integration is carried out for each edge which is visible from the source and the receiver. In the example in Fig. 1(c), only the four edges of the top surface of the box are visible from the source and the receiver. The numerical integration is done using Matlab's `QUADGK` function, with the addition of a series expansion of the integrand around the singular apex point, using a frequency-domain version of the method in [2]. Thus, the first-order diffraction term can be computed with a high accuracy at a reasonable computational cost. Finally, for the computation of the higher-order diffraction (HOD) term, an integral equation on a matrix form must be solved, as described in [3]. The integral equation, called the edge source integral equation, or ESIE, gives a set of edge source amplitudes, and from these, a propagated sound pressure can be computed at any external reveiver position. The integral equation, given in [3], is a Fredholm equation of the second kind, which can be solved with the Nystrom, or quadrature, method. An iterative method is used (the Neumann series approach), since a very large, sparse matrix needs to be inverted. The accuracy of the HOD-term depends on the quadrature order used, called "edge points" or "Gauss points", n_{gauss}, per edge in the following. The computation time for p_{HOD} depends on n_{gauss}^3 and therefore approaches to keep the n_{gauss} low are very attractive.

2.3. An illustrative example

One numerical challenge of the ESIE approach can be illustrated by a back-scatter example. A source and receiver were co-located at a distance of 10 m symmetrically above a square, thin plate of size 1m by 1m, in air with $c = 344$ m/s. The direct sound was left out here. Fig. 2 shows the resulting frequency response, illustrating the typical high-pass response for the reflection from a finite reflector. Also shown are the responses when only the specular reflection is included, and when first-order diffraction is included. It can be observed that first-order diffraction seems to suffice for medium-to-higher frequencies, whereas higher-order diffraction is absolutely necessary for lower frequencies. Furthermore, it can be seen that the quadrature order (ng, for n_{gauss}) per edge, for the higher-order diffraction seems to have a great impact for the very lowest frequencies, but much less so for slightly higher frequencies (above 10 Hz). It might seem surprising that the numerical accuracy of the HOD calculations has the strongest impact at the lowest frequencies, but it is a typical demonstration of loss of significance. The total field is a sum of three

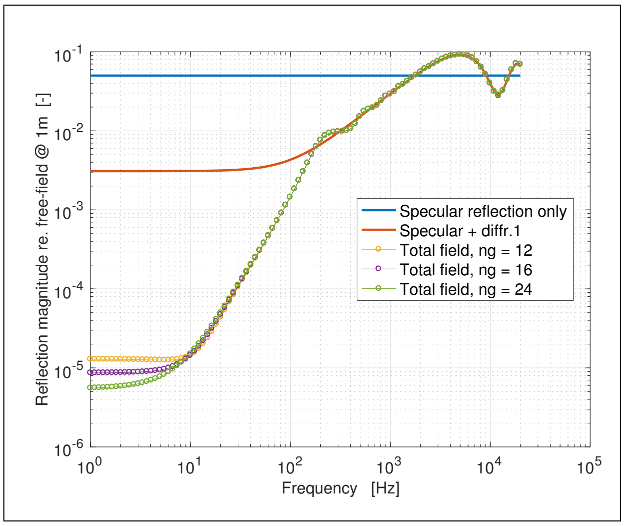

Figure 2. Back-scatter for a thin, rigid plate, 1m by 1m, from a distance of 10m.

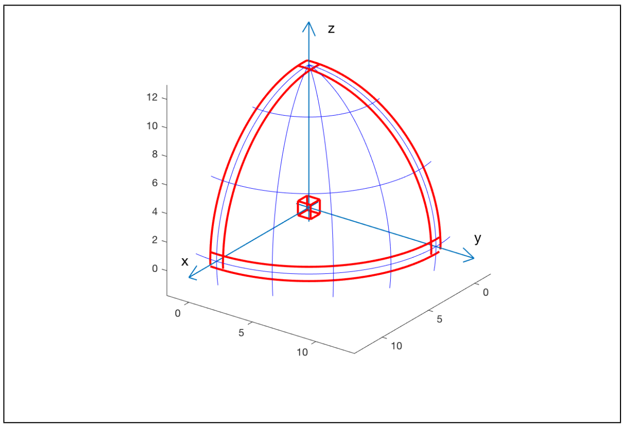

Figure 3. One octant of a spherical surface around a cube-shaped scattering object. The red arcs indicate source/receiver directions for which the higher-order diffraction integral kernel gets singular.

terms, see Eq. (1), and the magnitude of this sum is much smaller than the magnitude of the three involved terms. As a consequence, the relative error of the sum is much larger than the relative error of the three terms independently. The first two terms (p_{GA} and $p_{\mathrm{diffr.1}}$, respectively) are computed with very high accuracy, so it is the relative error of the third term, p_{HOD}, that dominates, and this term must be computed with higher and higher accuracy, the lower the frequency. Exactly that numerical challenge is a main topic of this paper, so in the results section, only results for those very low frequencies will be displayed.

2.4. Challenges for the ESIE method

As argued above, the required accuracy for the computation of p_{HOD} generally increases, the weaker the total field magnitude is. In addition, the calculation of p_{HOD} has challenges for certain source and receiver directions, [4], as well as for smooth scattering bodies that are represented as polyhedra. The challenge is that the kernel in the integral equation has a singularity for source/receiver directions that are very close to one of the infinite planes that the scatterer faces belong to. Fig. 3 illustrates these challenging directions for a cube-shape scatterer. Only one quadrant of the full space is shown, because of symmetry. The red arcs indicate source/receiver directions where the kernel directivity singularity is encountered. Regardless of source position, receivers close to those red arcs will encounter very slow convergence of the results for p_{HOD}.

2.4.1. Mitigation technique 1: Richardson extrapolation

For a numerical method that depends on some discretization with n points, a Taylor expansion model can be employed, assuming that the computed result with n points, $\hat{p}_n$, is the final sought result, p_{final}, plus some polynomial form for the error,

$$\hat{p}_n = p_{\mathrm{final}} + A\left(\frac{1}{n}\right)^B + \ldots$$

where the leading exponent B is either known from the method's numerical properties, or empirically derived. The unknowns, including the one of most interest, p_{final}, can be estimated based on a few computed values with different discretizations, assuming that those computations are in a range where the leading term is dominating the error. It has been demonstrated that the ESIE method used here, where a Gauss-Legendre quadrature approach is used, leads to $B = 2$ (except close to the challenging receiver positions shown in Fig. 3) . Thus, the potential exponential convergence for Gaussian quadrature is not fulfilled, since the integral kernel has endpoint singularities that limit the convergence. By plotting the computed values, $\hat{p}_n$ against $x_n = n_{\mathrm{gauss}}^{-2}$, the constant parameter (p-intercept) of a linear regression will be the estimate of p_{final}. Such extrapolated values can be found from different sets of computed datapoints, and these extrapolated values can in turn be used for another round of extrapolation, with a higher coefficient B for the error term. Here, only a first round of extrapolation will be demonstrated.

2.4.2. Mitigation technique 2: Combining the ESIE with the BEM

It has recently been suggested that the numerical problems with the ESIE for certain receiver positions can be avoided by combining the ESIE with the Helmholtz integral, in the same was as the boundary element method (BEM) uses the latter, [5]. Thus, the ESIE is used to compute the sound pressure at intermediate receiver positions across the surface of the scattering body. In a subsequent step, this surface sound pressure is propagated to an external receiver

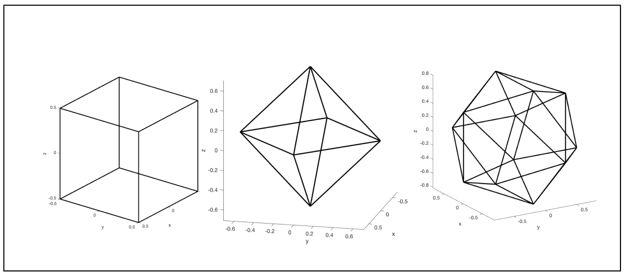

Figure 4. Three scattering objects: (a) Cube, (b) Octahedron, (c) Icosahedron

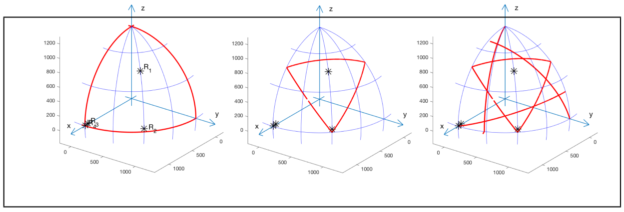

Figure 5. Four source/receiver positions for the (a) cube, (b) octahedral, and (c) icosahedral scatterers. Positions where the diffraction integral kernel is singular are indicated by the red arcs.

position, P (leaving out the direct sound, since we are interested in the backscatter case here),

$$p(P) = -\frac{1}{4\pi}\int p_{\mathrm{surf}}\frac{\mathrm{e}^{-\mathrm{j}kr}}{r}\left(\mathrm{j}k + \frac{1}{r}\right)\cos\varphi dS$$

computed numerically as

$$p(P) \approx -\frac{S_{\mathrm{total}}}{4\pi}\sum_{i=1}^{N} w_i p_{\mathrm{surf},i}\frac{\mathrm{e}^{-\mathrm{j}kr}}{r}\left(\mathrm{j}k + \frac{1}{r}\right)\cos\varphi$$

for the N intermediate surface receiver positions where the surface sound pressure has been computed with the ESIE. Here, a Gauss-Legendre quadrature product rule is used for quadrilateral faces, and quadrature rules from [6] for triangular faces, of the scattering polyhedron. S_{total} is the total surface area of the scattering body.

3. Examples

Three different scattering bodies are studied here, a cube, an octahedron, and a regular icosahedron, as illustrated in Fig. 4. They are scaled to the same volume, 1 m^3. A source and a receiver are co-located at a distance of 1000 m, for a few different source/receiver angles, so monostatic backscattering is studied here. For the cube example, Fig. 5(a) illustrates four source/receiver positions by crosses and labels R_i. The position R_1 is unproblematic, being far away from the polyhedron/cube planes, whereas positions R_2 to R_4 are close to one or two of those planes. Note that the distance to the scattering object is 1000 m here, which makes the two parallel planes that are visible in Fig. 3 collapse into one. Figs. 5(b) and (c) show corresponding challenging directions for the octahedral and icosahedral scatterers as well.

The monostatic backscatter amplitude was computed for the two frequencies 1 Hz and 10 Hz, with a speed of sound of 344 m/s. Three different diffraction-based methods were used: the basic ESIE with different values of n_{gauss} per edge, extrapolated ESIE (see section 2.4.1), and ESIEBEM (see section 2.4.2), with 5*5 quadrature points per cube face, following a product Gauss-Legendre rule, or 7 quadrature points per triangular face for the octahedron and icosahedron scatterers. The Matlab EDtoolbox was used for all these calculations, [7]. Reference results were also computed with the OpenBEM Matlab software [8], using meshes generated with the gmsh software, [10]. Those reference meshes have 17972, 16920, and 15318 nodes, respectively, for the three scatterers in Fig. 4.

4. Results

Figs. 6 and 7 show the backscatter magnitude for the cube scatterer, for the frequency 1 Hz ($kL \approx 0.018$), as function of number of gauss points per edge, for the two receiver positions 1 and 4. The results in Fig. 6 indicate that the extrapolated results based on the ESIE method converge quite well to the same values as the ESIEBEM and BEM results, but the ESIEBEM results need remarkably low numbers of gauss points, and a surface quadrature order of 5*5 per cube face seems to suffice for this low frequency. The ESIE results might seem to be very problematic since a convergence towards the reference BEM result can not be observed. However, for even higher values of gauss points per edge, the ESIE result do indeed tend towards the correct result. The large deviation is caused by the fact that the ESIE result passes through the origin, the value 0, in the complex plane, on its convergence trajectory towards the right result (not shown). Interestingly, the extrapolation detects such a trajectory and easily finds an accurate estimate of the final convergence value. By inspecting the results for the same source/receiver, but the frequency 10 Hz, in Fig. 8, one can observe perfectly expected convergence patterns. Please note the very different scales in Figs 6-fig$_c uberes4$.

The more problematic receiver R_4 leads to problems for the ESIE method, as seen in Fig. 7, and the results seem to converge very slowly towards the results of the ESIEBEM and BEM. Again, it seems like the ESIEBEM approach is much more robust and efficient. Also shown in Figs. 6 and 7 are the theoretical low-frequency values for the backscatter from a rigid, spherical scatterer,

$$|p_{LF,theo}| = \frac{5(ka)^2 \cdot a}{6}$$

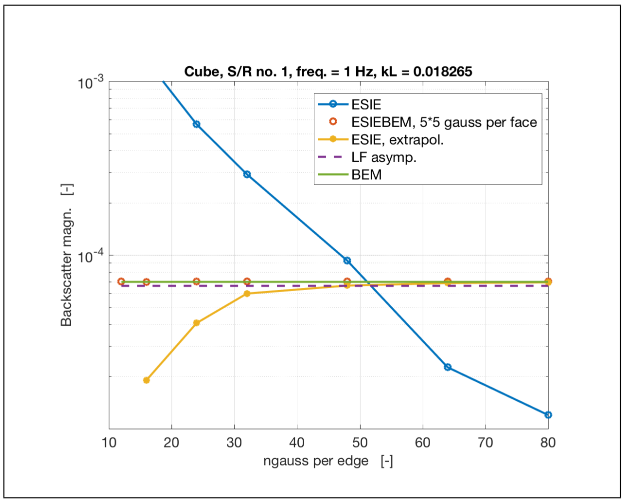

Figure 6. Backscatter amplitude for the cube scatterer at 1 Hz, as function of gauss points per edge for the unproblematic receiver R_1.

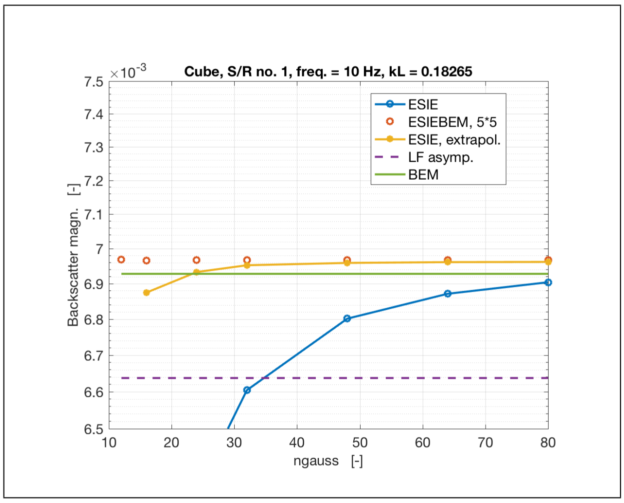

Figure 8. Backscatter amplitude for the cube scatterer at 10 Hz, as function of gauss points per edge for the unproblematic receiver R_1.

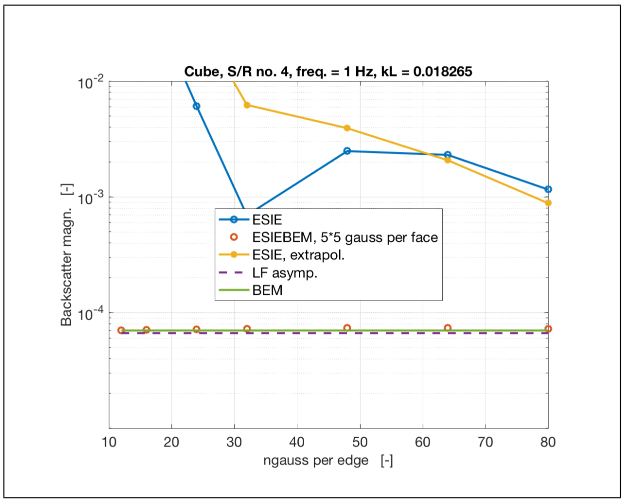

Figure 7. Backscatter amplitude for the cube scatterer at 1 Hz, as function of gauss points per edge for the problematic receiver R_4.

where a is the radius, and k is the wavenumber, [10]. For the polyhedral scatterers, we use an effective radius value, a, for which the sphere of that radius gets the same volume as the polyhedral object.

For both the octahedral and the icosahedral scattering objects in Fig. 4 (b) and (c), results follow the same trends as in Figs. 6 and 7. All results are compiled in the next subsection.

4.1. Compiled results

In Table I, the results for the ESIE method are compiled for the two frequencies, and all three scatterer bodies. Results have been divided into two types of receivers: unproblematic ones and problematic ones. The extrapolated ESIE results are presented in Table II. Some quite clear trends can be observed. First, the basic ESIE method has big problems for certain problematic receiver positions, as demonstrated by the huge errors in the lower half of Table I. Second, the basic ESIE method also has problems for the non-problematic receivers, for the lowest frequency, as seen in the upper half of Table I. The reason for the challenge at low frequencies was demonstrated in Fig. 2. The extrapolation technique seems to accelerate the convergence of the ESIE method, as intended, but there are limits to how well the extrapolation can perform. In the upper half of Table II, very good accuracy results for the non-problematic receivers. For the problematic receivers, some improvement can be observed, but it is apparently not enough to give useful results.

The ESIEBEM method has no challenging receiver directions, even though source directions near the dangerous directions in Fig. 5 will cause slower convergence for the ESIEBEM method as well. Table III gives the errors for the ESIEBEM method, for the source/receiver positions with the largest errors. Apparently, good accuracy is maintained for all three scatterer bodies, both frequencies, and all four source/receiver directions.

4.2. Backscatter of polyhedra vs. sphere

The backscatter values, computed with the robust ESIEBEM method, are compared with the theoretical value for a spherical scatterer in Fig. 9. Apparently, the icosahedral scatterer response is closer to the theoretical sphere response, than the cube response is, as expected.

5. CONCLUSIONS

Some of the most challenging examples for edge-diffraction based scattering modeling have been studied here: low-frequency backscatter from polyhedral bodies. Using BEM results as reference, it has been

Table I. Final results, for the highest number of gauss points ped edge (80), for the ESIE method, worst source/receiver position. Values are deviations in dB from reference BEM results. Values in parentheses have apparantly not converged to usefully accurate values.

ESIE method	1 Hz	10 Hz
Non-problematic receivers		
Cube	(5.2 dB)	0.06 dB
Octahedron	(3.3 dB)	0.17 dB
Icosahedron	(7.6 dB)	0.28 dB
Problematic receivers		
Cube	(38.0 dB)	(5.1 dB)
Octahedron	(37.0 dB)	(3.2 dB)
Icosahedron	(66.3 dB)	(26.8 dB)

Table II. Results for extrapolations of the ESIE results. Values are deviations in dB from reference BEM results. Values in parentheses have apparantly not converged to usefully accurate values.

ESIE extrapolation	1 Hz	10 Hz
Non-problematic receivers		
Cube	0.05 dB	0.01 dB
Octahedron	0.17 dB	0.04 dB
Icosahedron	0.18 dB	0.01 dB
Problematic receivers		
Cube	(4.2 dB)	0.07 dB
Octahedron	(33.4 dB)	(1.3 dB)
Icosahedron	(38.5 dB)	(5.5 dB)

Table III. Final results for the ESIEBEM method, for the worst source/receiver position. Values are deviations in dB from reference BEM results.

ESIEBEM	1 Hz	10 Hz
Cube	0.28 dB	0.10 dB
Octahedron	0.05 dB	0.07 dB
Icosahedron	0.24 dB	0.07 dB

confirmed that the basic ESIE method has some challenges with these examples. The problems are both caused by some challenging source/receiver positions and because of extreme accuracy requirements for the computation of higher-order diffraction at very low frequencies. The extrapolation of ESIE results has been demonstrated to lead to significant improvement in accuracy, but does not help for challenging receiver directions. The ESIEBEM method, on the other hand, seems to avoid both the challenging receiver directions and the extreme accuracy requirements at low frequencies.

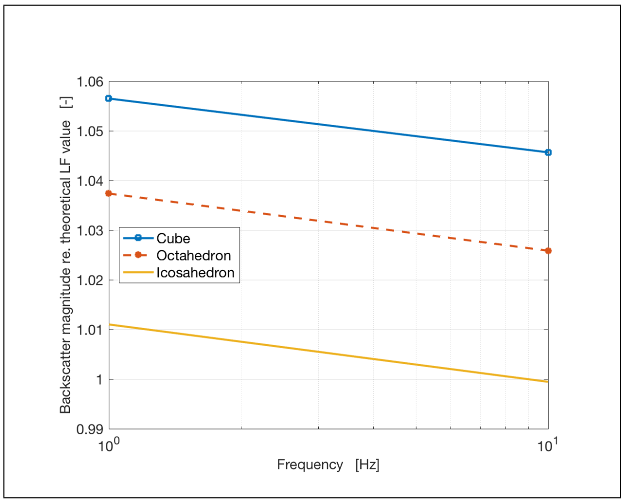

Figure 9. Backscatter amplitude for the three scatterers, as computed with the ESIEBEM method, compared with the theoretical LF response of a spherical scatterer.

References

[1] U. P. Svensson, P. T. Calamia, S. Nakanishi: Frequency-domain edge diffraction for finite and infinite edges. Acta Acustica united with Acustica 95 (2009) 568-572.

[2] U. P. Svensson, P. T. Calamia: Edge-diffraction impulse responses near specular- and shadow-zone boundaries. Acta Acustica united with Acustica 92 (2006) 501-512.

[3] A. Asheim, U. P. Svensson: An integral equation formulation for the diffraction from convex plates and polyhedra. Journal of the Acoustical Society of America 133 (2013) 3681-3691.

[4] U. P. Svensson, H. Brick, J. Forssén: Benchmark cases in 3d diffraction with different methods. In: Proceedings of the 7th Forum Acusticum, Krakow, Poland (2014).

[5] S. R. Martin, U. P. Svensson, J. Slechta, J. O. Smith: A hybrid method combining the edge source integral equation and the boundary element method for scattering problems. In: Proceedings of Meetings on Acoustics. **26**(1), 015001 (2016), doi:10.1121/2.0000226.

[6] D. A. Dunavant: High degree efficient symmetrical Gaussian quadrature rules for the triangle. Int. Journal for Numerical Methods in Engineering 21 (1985) 1129-1148.

[7] EDtoolbox, avaialable at github.com.

[8] OpenBEM, avaialable at openbem.dk.

[9] C. Geuzaine, J.-F. Remacle: Gmsh: a three-dimensional finite element mesh generator with built-in pre- and post-processing facilities. Int. Journal for Numerical Methods in Engineering 79 (2009) 1309-1331.

[10] E. G. Williams: Fourier Acoustics. Academic Press, London, 1999.